Olivares-Sánchez-Mellado, I.; Sanchis Kilders, P. (2021). A SiGe Slot Approach for Enhancing Strain Induced Pockels Effect in the Mid-IR Range. IEEE Photonics Technology Letters. 33(16):848-851. https://doi.org/10.1109/LPT.2021.3075753

A SiGe slot approach for enhancing strain induced Pockels effect in the mid-IR range

Irene Olivares, and Pablo Sanchis, *Senior, IEE,*

***Abstract*—Strained silicon was proposed more than a decade ago promising to revolutionize the silicon photonics field by allowing efficient modulation in this platform. Despite all the efforts, still rather low $\chi(2)$ values have been measured in strained silicon devices. In addition, the way of applying strain has not barely changed since the concept was proposed, usually consisting on a silicon waveguide covered by a stressor material such as silicon nitride. In this letter, a SiGe slot approach is explored as a different route to enhance the strain induced Pockels effect in the mid-IR range. Such approach would allow effective index change values which are near to 10^{-4} and improve the values expected for the most common silicon - silicon nitride structure by more than three orders of magnitude.**

***Index Terms*—strained silicon, Pockels effect, SiGe**

I. Introduction

THE strained silicon field was born in 2006 when low-frequency electro-optic modulation was measured in a strained silicon photonic crystal Mach-Zehnder interferometer [1]. Due to the observed linear relationship between the applied voltage and the effective index change, the modulation was attributed to Pockels effect, estimating a induced strain $\chi^{(2)}$ of ∼15 pm/V. In view of the results, it was proposed that the silicon nitride deposited on top of the waveguide was straining the silicon and, in this manner, was breaking the centrosymmetry of its lattice. The possibility of enabling Pockels effect in silicon opened the door to a new route for achieving efficient and fully CMOS compatible modulation in a simple and cost-effective way. Following studies improved even more the obtained results, reaching second order non-linearities as large as ∼ 340 pm/V in 2014 [2]. They were mostly focused on enhancing the Pockels effect by optimizing strain and waveguide geometry [3], [4], [5]. Despite the encouraging initial findings, subsequent studies started to question if Pockels effect was really the underlying mechanism behind the measured responses. In fact, published works studying second harmonic generation in strained silicon waveguides pointed to much lower values of $\chi^{(2)}$ in the order of several pm/V [6].Moreover, the strong influence of plasma dispersion effect in the obtained results was later demonstrated by Azadeh et. al. in 2015[7] and corroborated as well by many other experimental works [8], [9], [10]. The influence of the trapping properties of the silicon nitride cover layer was also demonstrated [11] and, regarding the second harmonic experiments, it was proposed that the measured non-linear responses could have arisen not from the silicon material itself but rather from the cover layer [12] or due to the trapped charges inside it [13]. Therefore, all the experimental evidence suggested that the Pockels effect was much weaker than initially thought. From a thoretical perspective, a new model based on the bond orbital description of the silicon covalent bond was published [14], predicting values of $\chi^{(2)}$ around several pm/V. More recently, high frequency modulation was demonstrated in a strained Mach-Zehnder interferometer showing a coherent response with the bond orbital model [15]. Nevertheless, the extracted value for the strain induced $\chi^{(2)}$ was of 1.8 pm/V, still pointing to a rather weak Pockels effect.

It is clear, therefore, that Pockels effect should be enhanced to achieve efficient modulation in strained silicon. With this aim, a p-i-n junction was proposed in our previous work [16] to tackle the main problems hindering Pockels effect, improving the effective index change values in a factor of 200 compared to the most common silicon-silicon nitride waveguide structure. Furthermore, the way of applying strain, mainly using a stressing silicon nitride cover, has not barely changed since the concept of strained silicon was proposed [17], [2], [7], [8], [11], [18], [15]. This situation contrasts when compared to the microelectronic industry, where a much diverse variety of methods for applying strain can be found, [19], [20]. More specifically, the use of silicon-germanium alloys ($Si_{1-x}Ge_x$) to apply strain is a mature technique employed to tune the electrical and optical properties of silicon and other materials. For example, in reverse embedded-SiGe MOSFETs the elastic relaxation of a buried compressive SiGe layer is used to induce tensile strain in the silicon. In this manner, it is possible to enhance, among others, the carrier mobilities in the channel [21]. In this line, our last work explored a SiGe-Si-SiGe structure [22] to increase the strain gradients inside the silicon layer, improving at the same time their overlap with the optical mode. In this letter, we follow the same approach but replacing the silicon layer by a three layer stack consisting in two SiGe layers ($Si_{0.35}Ge_{0.65}$ and $Si_{0.65}Ge_{0.35}$) plus the silicon film, all of them sandwiched between two thick germanium layer. The resulting effective index change of the guided mode is improved in more than three orders of magnitude compared to the one obtained in conventional silicon waveguides covered with a highly stressed silicon nitride layer. However, the operation regime is located at mid-IR wavelengths due to the use of Germanium.

II. The SiGe slot structure

The proposed device consists on a layered structure grown on a (100) silicon SOI wafer. The bottom and top Germanium layers have been chosen to be 200 nm thick. Sandwiched between them, a three layer stack will be epitaxially grown.

Manuscript received February 8, 2021; revised – –, –.

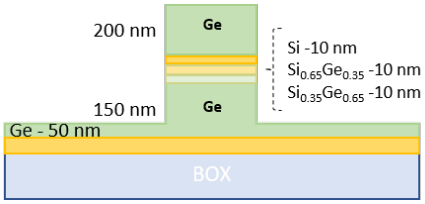

Fig. 1. The proposed Ge-SiGe-Si-Ge slot structure

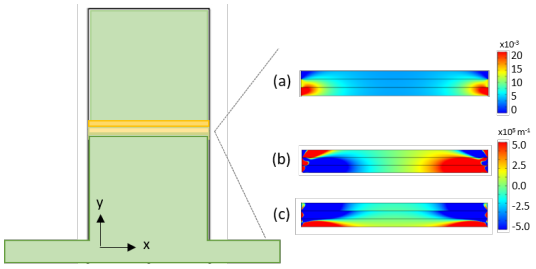

Fig. 2. Contour plot of the (a) ε_{xx} strain component and the (b) horizontal $\frac{\partial \varepsilon_{xx}}{\partial x}$ and (c) vertical $\frac{\partial \varepsilon_{xx}}{\partial y}$ strain gradients for ε_{xx} in the strained Si-SiGe stack.

The main goal is to have a highly stressed silicon film but, in order to do that, a smooth transition is needed between the germanium and silicon because, if the lattice mismatch is too large, dislocations in the interface will appear and no stress will be transferred to the silicon film. Therefore, two SiGe films are epitaxially grown from the Ge bottom layer with x=0.65 and x=0.35 germanium concentrations, respectively. The silicon layer is then grown on top of them. A thickness of 10 nm has been chosen for the three layers taking into account the critical thickness to avoid the formation of misfit dislocations [23]. A fully relaxed 200 nm thick Ge top layer is finally grown on top of the silicon with the aim of having an inhomogenous strain. Moreover, there is no need for the Ge top layer to be in its crystalline state because it is not intended to apply strain to the silicon film, thefore, the growth of an amorphous Ge layer could be explored, if needed, to ease the fabrication process. The design has been carried out in the 2 μm region for low loss operation. A sketch of the designed structure is shown in Fig. 1.

III. Strain Applied to the Si-SiGe Stack

The strain due to the SiGe layers has been simulated with SILVACO Athena and Atlas software packages [24] and it is dependent on the Ge concentration of each layer. Values near to 10^{-2} for the strain are found inside the three layer stack, as it can be observed in Fig. 2 (a), and even higher in the edges due to the effect of the etching process. Such values are around one order of magnitude more intense than those of the silicon-silicon nitride waveguide configuration. Moreover, the strain gradients reach values about 10^5 m^{-1}, as depicted in Fig. 2 for the (b) $\frac{\partial \varepsilon_{xx}}{\partial x}$ and (c) $\frac{\partial \varepsilon_{xx}}{\partial y}$ components. But even more interesting is the fact that the vertical $\frac{\partial \varepsilon_{xx}}{\partial y}$ strain gradients in Fig. 2 (c) are mainly negative, as opposed to what happens for $\frac{\partial \varepsilon_{xx}}{\partial x}$ in Fig. 2 (b). In this case, the horizontal strain gradient shows a completely anti-symmetric distribution, with areas of opposite sign canceling each other out. In fact, this was one of the main issues observed in the silicon-silicon nitride waveguides, as also discussed in other published studies [22]. The three-layer SiGe stack, therefore, aids to avoid the appearing of counteracting strained areas.

IV. Electric Field Strength Inside the Strained Silicon Layer

To simulate the electrical behavior of the device, the correct values for the $Si_{1-x}Ge_x$ alloys must be considered. Most of optical and electrical parameters follow a linear relationship with concentration, which is the case of the band gap and dielectric constant [25].

TABLE I
Si and $Si_{1-x}Ge_x$ material parameters at 2 μm

	parameter	*units*	*value*
Silicon	Refractive index		3.451
	Band Gap	eV	1.12
	Electron affinity	eV	4.05
	Dielectric constant		11.9
$Si_{0.65}Ge_{0.35}$	Refractive index		3.680
	Band Gap	eV	0.959
	Electron affinity	eV	4.032
	Dielectric constant		13.34
$Si_{0.35}Ge_{0.65}$	Refractive index		3.875
	Band Gap	eV	0.851
	Electron affinity	eV	4.018
	Dielectric constant		14.57
Ge	Refractive index		4.104
	Band Gap	eV	0.66
	Electron affinity	eV	4.0
	Dielectric constant		16.0

Therefore, they have been obtained by interpolating from pure Si and Ge values. Table I summarizes the parameters used in the simulations.

To obtain the results, the voltage (Vg) has been applied to the top Ge layer while the bottom has been grounded. The resulting electric field in the whole structure for an applied voltage of 12V is shown in Fig. 3(a) together with the (b) horizontal and (c) vertical components inside the three layer stack. Moreover, Fig. 3(d) shows also E_y along the vertical line marked in Fig. 3(a) to show the electric field values inside the structure. In fact, the maximum voltage that can be applied to the device is limited at 12 V and -5 V at positive and negative voltages, respectively, by the breakdown field of germanium (12.5 V/μm [26]). The breakdown field for Ge is also marked in Fig. 3(d) as indication. It is possible to observe in the images of Fig. 3 how the heterojunction helps to concentrate the electric field inside the silicon. While a gradual rise on the electric field values can be observed in Ge, a steep increase happens at the Si and SiGe layers, reaching maximum electric fields of around ±17 V/μm in the silicon film. Hence, the higher electric field intensity located in the strained silicon layer will further contribute to enhance Pockels effect. In addition, it is important to highlight the asymmetric behavior between positive and negative voltages, obtaining higher electric fields for negative applied biases and,

therefore, reaching the limit due to the germanium breakdown field at lower values. This behavior will also be reflected in the relationship between refractive index change and applied voltage, as we will see in the following.

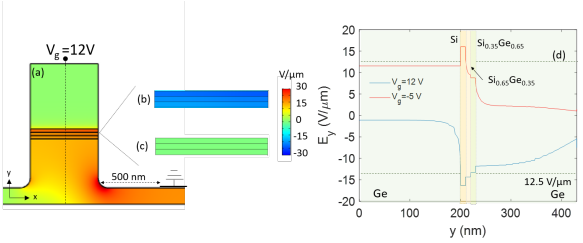

Fig. 3. (a) Electric field norm for the whole structure and (b) E_x and (c) E_y components in the strained Si-Ge stack at 12V. (d) Values of the E_y component along the vertical line depicted in (a).

V. The Strain Induced Effective Index Change

Thanks to the smaller refractive index of Si and SiGe films compared to that of germanium, the guided optical mode is mainly concentrated in the strained stack, as it is shown in Fig. 4 (a). The propagation losses of the optical mode are below 1 dB/cm at the considered 2 μm wavelength. The refractive index change of silicon has been calculated for an applied voltage of 12 V, taking into account the bond orbital model [14], where the same values for the experimental parameters α and β determined in [18] at 1.55 μm have been considered as an approximation. The results for the Δn_{yy} are depicted in Figure 4 (b), where values even larger than 10^{-4} can be observed. However, germanium is also a centrosymmetric material which lacks $\chi^{(2)}$ non-linearities due to the inversion symmetry of its lattice. The highly strained SiGe layers, therefore, could also contribute in a similar way as silicon to the final effective index change. Furthermore, the effect of those layers should be analyzed in order to know how they can affect the device performance. Hence, the refractive index for the SiGe films has also been calculated, approximating the same α and β values as those for silicon. In addition, a value of 0.5 has been used for the S parameter, related to the overlap between hybrid orbitals. The values for the bond length and γ have been interpolated considering those of pure silicon (d=0.235 nm, γ=1.4 [14]) and germanium (d=0.245 nm, γ=1.6 [27]). The Δn_{yy} for the three layers is depicted in Fig. 4 (c).

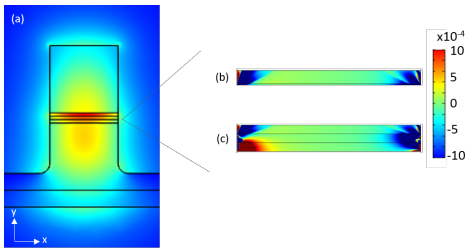

Fig. 4. (a) Optical mode and n_{yy} refractive index change for (b) silicon and (c) the three Si-SiGe stack.

Then, the effective index change of the optical mode has been calculated considering two scenarios: one in which only the silicon film contributes to the final effective index change and another in which the three layers are considered. The results are shown in Fig. 5, where it is possible to see that the best outcomes are obtained when the Si plus the two SiGe layers are taken into account. A smaller effective index change is obtained when only silicon is considered, in which a total value of $\sim 3{\cdot}10^{-5}$ is obtained when a sweep between -5 V and 12 V is performed. Again, an asymmetric behavior for positive and negative voltages is observed for the effective index change as a consequence of the asymmetry in the electric field already described in the precious section. On the other hand, more encouraging outcomes are obtained when the three layers are considered. In this case, a total index change of $\sim 7{\cdot}10^{-5}$ is achieved. This result improves in more than three ordes of magnitude the expected results for the usual silicon-silicon nitride structure and by around 12 times the results obtained using a p-i-n junction with an asymmetric stress cladding as proposed in our previous work [22].

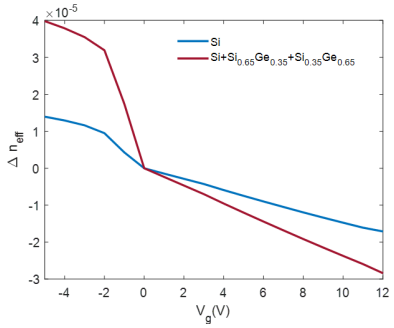

Fig. 5. Effective index change as a function of the applied voltage considering the contribution of silicon (blue) and silicon plus both SiGe layers (red).

VI. Conclusion

The values of the effective index change obtained with the Si-SiGe structure suppose a clear step forward in the progress towards efficient modulation based of strain induced Pockels effect. On one hand, they would hugely facilitate the experimental demonstration of Pockels effect in strained silicon and, if proven, could mark a milestone in the silicon photonics field. Hence, the Pockels effect could be exploited with the discussed structure, reaching an effective index change near to 10^{-4}. The proposed device has been designed to work at the beginning of the mid-IR range, at around 2 μm, however, whenever experimental values for the α and β parameters of the bond orbital model are available at higher wavelengths, the same design could be extended at higher wavelengths in the mid-IR range. Therefore, the silicon-germanium system allows to efficiently strain the silicon layer possibiliting, at the same time, a high electric and optical field overlap. In addition, the SiGe system is a mature technique employed both, in electronic and photonics, broadly used to engineer structures such as MOSFETs [21], light-emitting diodes [28] or single-electron quantum devices [29]. Moreover, very recently efficient direct-bandgap emission has been achieved in SiGe alloys [30] making this material system an ideal platform

for combining electronic and photonic devices in the same chip.

ACKNOWLEDGMENT

This work is supported by Ministerio de Ciencia e Innovación (TEC2016-76849, PID2019-111460GB-I00) and Generalitat Valenciana (PROMETEO/2019/123).

REFERENCES

[1] R. S. Jacobsen, K. N. Andersen, P. I. Borel, J. Fage-Pedersen, L. H. Frandsen, O. Hansen, M. Kristensen, A. V. Lavrinenko, G. Moulin, H. Ou *et al.*, "Strained silicon as a new electro-optic material," *Nature*, vol. 441, no. 7090, pp. 199–202, 2006.

[2] P. Damas, X. Le Roux, D. Le Bourdais, E. Cassan, D. Marris-Morini, N. Izard, T. Maroutian, P. Lecoeur, and L. Vivien, "Wavelength dependence of pockels effect in strained silicon waveguides," *Optics Express*, vol. 22, no. 18, pp. 22 095–22 100, 2014.

[3] B. Chmielak, M. Waldow, C. Matheisen, C. Ripperda, J. Bolten, T. Wahlbrink, M. Nagel, F. Merget, and H. Kurz, "Pockels effect based fully integrated, strained silicon electro-optic modulator," *Optics Express*, vol. 19, no. 18, pp. 17 212–17 219, 2011.

[4] F. Bianco, K. Fedus, F. Enrichi, R. Pierobon, M. Cazzanelli, M. Ghulinyan, G. Pucker, and L. Pavesi, "Two-dimensional micro-Raman mapping of stress and strain distributions in strained silicon waveguides," *Semiconductor Science and Technology*, vol. 27, no. 8, p. 085009, 2012.

[5] C. Schriever, C. Bohley, and R. B. Wehrspohn, "Strain dependence of second-harmonic generation in silicon," *Optics letters*, vol. 35, no. 3, pp. 273–275, 2010.

[6] M. Cazzanelli, F. Bianco, E. Borga, G. Pucker, M. Ghulinyan, E. Degoli, E. Luppi, V. Véniard, S. Ossicini, D. Modotto *et al.*, "Second-harmonic generation in silicon waveguides strained by silicon nitride," *Nature Materials*, vol. 11, no. 2, pp. 148–154, 2012.

[7] S. S. Azadeh, F. Merget, M. Nezhad, and J. Witzens, "On the measurement of the Pockels effect in strained silicon," *Optics Letters*, vol. 40, no. 8, pp. 1877–1880, 2015.

[8] R. Sharma, M. W. Puckett, H.-H. Lin, A. Isichenko, F. Vallini, and Y. Fainman, "Effect of dielectric claddings on the electro-optic behavior of silicon waveguides," *Optics Letters*, vol. 41, no. 6, pp. 1185–1188, 2016.

[9] M. B. Borghi, M. M. Ancinelli, F. M. Erget, J. W. Itzens, M. B. Ernard, M. G. Hulinyan, G. P. Ucker, and L. P. Avesi, "High-frequency electro-optic measurement of strained silicon racetrack resonators," *Optics Letters*, vol. 40, no. 22, pp. 5287–5290, 2015.

[10] M. Borghi, M. Mancinelli, M. Bernard, M. Ghulinyan, G. Pucker, and L. Pavesi, "Homodyne Detection of Free Carrier Induced Electro-Optic Modulation in Strained Silicon Resonators," *Journal of Lightwave Technology*, vol. 34, no. 24, pp. 5657–5668, 2016.

[11] I. Olivares, T. Angelova, and P. Sanchis, "On the influence of interface charging dynamics and stressing conditions in strained silicon devices," *Scientific Reports*, vol. 7, no. 1, pp. 1–8, 2017.

[12] J. B. Khurgin, T. H. Stievater, M. W. Pruessner, and W. S. Rabinovich, "On the origin of the second-order nonlinearity in strained Si–SiN structures," *JOSA B*, vol. 32, no. 12, pp. 2494–2499, 2015.

[13] C. Castellan, R. Franchi, S. Biasi, M. Bernard, M. Ghulinyan, and L. Pavesi, "Field-induced nonlinearities in silicon waveguides embedded in lateral pn junctions," *Frontiers in Physics*, vol. 7, p. 104, 2019.

[14] P. Damas, D. Marris-Morini, E. Cassan, and L. Vivien, "Bond orbital description of the strain-induced second-order optical susceptibility in silicon," *Physical Review B*, vol. 93, no. 16, p. 165208, 2016.

[15] M. Berciano, G. Marcaud, P. Damas, X. Le Roux, P. Crozat, C. A. Ramos, D. P. Galacho, D. Benedikovic, D. Marris-Morini, E. Cassan *et al.*, "Fast linear electro-optic effect in a centrosymmetric semiconductor," *Communications Physics*, vol. 1, no. 1, pp. 1–9, 2018.

[16] I. Olivares, J. Parra, A. Brimont, and P. Sanchis, "Enhancing pockels effect in strained silicon waveguides," *Optics express*, vol. 27, no. 19, pp. 26 882–26 892, 2019.

[17] R. S. Jacobsen, K. N. Andersen, P. I. Borel, J. Fage-Pedersen, L. H. Frandsen, O. Hansen, M. Kristensen, A. V. Lavrinenko, G. Moulin, H. Ou *et al.*, "Strained silicon as a new electro-optic material," *Nature*, vol. 441, no. 7090, pp. 199–202, 2006.

[18] P. Damas, M. Berciano, G. Marcaud, C. Alonso Ramos, D. Marris-Morini, E. Cassan, and L. Vivien, "Comprehensive description of the electro-optic effects in strained silicon waveguides," *Journal of Applied Physics*, vol. 122, no. 15, p. 153105, 2017.

[19] R. A. Minamisawa, M. J. Süess, R. Spolenak, J. Faist, C. David, J. Gobrecht, K. K. Bourdelle, and H. Sigg, "Top-down fabricated silicon nanowires under tensile elastic strain up to 4.5%," *Nature communications*, vol. 3, no. 1, pp. 1–6, 2012.

[20] C. K. Maiti and T. Maiti, *Strain-Engineered MOSFETs*. CRC Press, 2012.

[21] J. G. Fiorenza, J.-S. Park, and A. Lochtefeld, "Detailed simulation study of a reverse embedded-sige strained-silicon mosfet," *IEEE Transactions on Electron Devices*, vol. 55, no. 2, pp. 640–648, 2008.

[22] I. Olivares and P. Sanchis, "Enhanced pockels effect in strained silicon by means of a sige/si/sige slot structure." IEEE Photonics Conference (IPC), 2020, pp. 1–2.

[23] G. Abstreiter, K. Eberl, E. Friess, W. Wegscheider, and R. Zachai, "Silicon/germanium strained layer superlattices," *Journal of Crystal Growth*, vol. 95, no. 1-4, pp. 431–438, 1989.

[24] SILVACO, *International, 4701 Patrick Hnry Drive, Bldg 1, Sant Clara, California 94054, USA*. www.silvaco.com, 1984.

[25] M. E. Levinshtein, S. L. Rumyantsev, and M. S. Shur, *Properties of Advanced Semiconductor Materials: GaN, AIN, InN, BN, SiC, SiGe*. John Wiley & Sons, 2001.

[26] J. Liu, D. Pan, S. Jongthammanurak, K. Wada, L. C. Kimerling, and J. Michel, "Design of monolithically integrated gesi electro-absorption modulators and photodetectors on an soi platform," *Optics Express*, vol. 15, no. 2, pp. 623–628, 2007.

[27] W. A. Harrison, *Electronic structure and the properties of solids: the physics of the chemical bond*. Courier Corporation, 2012.

[28] D. D. Cannon, J. Liu, D. T. Danielson, S. Jongthammanurak, U. U. Enuha, K. Wada, J. Michel, and L. C. Kimerling, "Germanium-rich silicon-germanium films epitaxially grown by ultrahigh vacuum chemical-vapor deposition directly on silicon substrates," *Applied Physics Letters*, vol. 91, no. 25, p. 252111, 2007.

[29] S. Goswami, K. Slinker, M. Friesen, L. McGuire, J. Truitt, C. Tahan, L. Klein, J. Chu, P. Mooney, D. W. Van Der Weide *et al.*, "Controllable valley splitting in silicon quantum devices," *Nature Physics*, vol. 3, no. 1, pp. 41–45, 2007.

[30] E. M. Fadaly, A. Dijkstra, J. R. Suckert, D. Ziss, M. A. van Tilburg, C. Mao, Y. Ren, V. T. van Lange, K. Korzun, S. Kölling *et al.*, "Direct-bandgap emission from hexagonal ge and sige alloys," *Nature*, vol. 580, no. 7802, pp. 205–209, 2020.

Irene Olivares received the B.S. degree in physics from Complutense University, Madrid, Spain, in 2014 and the M.S. degree in renewable energies from the Complutense University, Madrid, Spain in 2015. She is pursuing the Ph.D. degree in telecommunication engineering at Politècnica University, Valencia, Spain. Her research interest includes the development and design of photonic integrated circuits and has especially worked in the topic of strained silicon. She has also been researching in the area of phase change materials.

Pablo Sanchis received the PhD degree from the Universitat Politècnica in 2005. He is Full-Professor at the same university since 2016. His research career has been developed at the Nanophotonics Technology Center where he leads a research group. His research interests are basically related with the design, fabrication and characterization of photonic integrated circuits, especially in the field of silicon photonics. He has authored more than 80 papers in peer-reviewed international journals and more than 140 papers in international conferences and he holds several patents. He has also been part of the organization committee of ECOC, ECIO, and other international conferences.